JOURNAL OF COMPUTATIONAL PHYSICS 33, 185–203 (1979)

Two Scaling Transformations for the Numerical Computation of Multidimensional Unsteady Laminar Flames

P. J. O'ROURKE AND F. V. BRACCO

Department of Mechanical and Aerospace Engineering, Princeton University, Princeton, New Jersey

Received August 4, 1978; revised December 20, 1978

Numerical computations of the unsteady propagation of multidimensional laminar flames are difficult to perform because the structure of the flame must be resolved and the thickness of the flame is often several orders of magnitude smaller than the characteristic dimension of the field. Two scaling transformations are discussed which make possible such computations by reducing the computation time to acceptable levels. The α-transformation is associated with the spatial uniformity of the time-varying pressure and is shown to be valid for low-Mach-number flows. It reduces computational time by either reducing the total number of time steps or, in the RICE code, the number of iterations required each time step. The β-transformation is related to the small thickness of the flame with respect to the characteristic dimension of the field and is shown to be useful for high Reynolds number flows. It reduces computation time by reducing the number of necessary grid points which, in turn, is achieved by broadening the flame front without altering the flame speed. The β-transformation was introduced by T. D. Butler and P. J. O'Rourke ("Proceedings, Sixteenth Symposium on Combustion, August 1976," pp. 1403–1516, The Combustion Institute, Pittsburgh, 1977). The validity of the two transformations is shown theoretically and through a series of computer calculations.

INTRODUCTION

In this paper, two scaling transformations are introduced which make possible the numerical computation of unsteady, multidimensional laminar flame propagation in premixed charges. A "flame," also called a deflagration, is a low-speed wave supported by exothermic chemical reactions [1]. Because complex geometries and complicated chemical kinetic rate dependencies are usually associated with prediction of flame propagation in practical systems, numerical solution is required. Numerical solution is, in turn, made difficult by two properties of laminar flames. First, typical Mach numbers are very small, of the order of 0.01 or less. Second, the thickness of the laminar flame is typically much smaller than the dimensions of the physical region of interest. Equivalently, one can say the Reynolds number based on a characteristic dimension of the combustion chamber is very large.

The scaling transformations allow one to use traditional Eulerian, compressible flow computer codes to solve multidimensional and unsteady problems with laminar flames. These traditional codes must compute with a time step which resolves the

0021-9991/79/110185–19$02.00/0

acoustic wave motion. In low Mach number flows, there is a great disparity between this time step and the larger time scales for changes in other features of the flow field. Much computational time is wasted in resolving the acoustic motion, whose only effect on the flow is to maintain a nearly uniform pressure in space. The α-transformation, that is one of the two transformations discussed in this paper, shows that when the Mach number is small, the dependent and independent variables can be scaled in such a way that the solution is unaffected, except for being scaled in time. By increasing the propagation speed of the computed flame by a factor of α, the disparity between the time scales for acoustic wave motion and laminar flame propagation is reduced, but the essential property that there is such a disparity is preserved by setting an upper bound on the value of α. An Eulerian computer code must also use the same computational cell size outside the flame, where it is not needed, that is used to resolve the flame front. The β-transformation, which is the second transformation to be discussed, shows that when the Reynolds number is large, the dependent and independent variables can be scaled in such a way that the solution is unaffected, except that the flame zone thickness is increased by a factor β. The disparity between the space scales inside and outside the flame zone is lessened. Again, by not choosing β too large, the essential property that there is such a disparity is preserved.

Classically, vanishingly small Mach numbers or very large Reynolds numbers have been used to simplify the equations, either, in the first case, by a formulation of the equations of motion which ignores acoustic waves, or, in the second case, by boundary-layer approximations. The resulting equations are simpler in appearance, but their numerical solution is still difficult. The approach followed in this work is different. It will be shown that considerable computational efficiency can be gained by retaining the full equations and scaling the Mach number to a larger (but not too large) value and the Reynolds number to a smaller (but not too small) value. In compressible boundary-layer theory, a transformation which is frequently used and which resembles the β-transformation is the Howarth transformation [2]. The Howarth transformation has a definite form and the motivation for its use is to simplify the equations so that an analytical solution can be obtained. The β-transformation induces spatial distortion like the Howarth transformation, but is more general in that β can be chosen in many ways, and the motivation for its use is to thicken the computed flame to facilitate the obtainment of numerical solutions. The β-transformation is also similar in concept to the artificial viscosity of von Neumann and Richtmyer [3] for the computation of hydrodynamic shock waves. But it satisfies the additional constraint of preserving the structure of the flame to obtain the correct flame speed [1]. To calculate the correct shock speed, it is only necessary to satisfy the jump conditions across it.

For the computation of multidimensional laminar flames, methods other than the α- and β-transformations have been proposed, but they present limitations and have not yet been successfully tested. An alternative to the α-transformation is the numerical solution of the equations governing low-speed flows, which neglect acoustic wave motion. One such equation set is given in the section on the derivation of the α-

transformation. But these equations are elliptic in nature, and numerical solution of elliptic equations can be very time consuming. For example, the ICE method [4], used in the calculation of this paper, reduces in the limit of low Mach number flow to the well-known MAC method [5] for incompressible flows. Yet, as will be seen, solving the equations with unscaled variables using ICE takes significantly more time than solving them using the α-transformation. An alternative to the β-transformation is the use of an adaptive grid scheme, such as in the ALE [6] technique, to provide finer resolution in the flame zone. To date, the complexity of using such a procedure in more than one space dimension has not been surmounted.

In the following section, we will describe the α- and β-transformations in more detail. Their theoretical justification and the conditions under which they are valid will be presented. Next, the results of a series of numerical calculations of laminar flame propagation in a premixed methane–air charge will be detailed. The purpose of the calculations is to show that the two transformations do indeed exhibit the expected properties when the conditions for their validity are respected and break down when they are not.

Derivation of the Scaling Laws

For future reference, we state here the equations of change for a chemically reacting mixture of ideal gases. The assumption of constant and equal specific heats of all species is made in order to simplify the equations, although it in no way affects the results we will derive. Continuity equation for species k:

$$\frac{\partial \rho_k}{\partial t} + \nabla \cdot (\rho_k \mathbf{u}) = \nabla \cdot (\rho D \nabla \rho_k/\rho) + W_k \sum_i R_i(\nu''_{k,i} - \nu'_{k,i}),$$
$$\rho = \sum_k \rho_k ; \tag{1}$$

Mixture momentum equation

$$\frac{\partial \mathbf{u}}{\partial t} + \mathbf{u} \cdot \nabla \mathbf{u} + 1/\rho \nabla p = 1/\rho \nabla \cdot \underline{\tau},$$
$$\underline{\tau} = \mu(\nabla \mathbf{u} + (\nabla \mathbf{u})^T] + \lambda \nabla \cdot \mathbf{u}\underline{\mathbf{I}}; \tag{2}$$

Mixture energy equation

$$\frac{\partial \rho h}{\partial t} + \nabla \cdot (\rho \mathbf{u} h) = \frac{\partial p}{\partial t} + \mathbf{u} \cdot \nabla p + \nabla \cdot (K \nabla T) + \underline{\tau} : \nabla \mathbf{u} + \sum_i R_i Q_i ; \tag{3}$$

Equations of state

$$p = \frac{\gamma - 1}{\gamma} \rho h, \tag{4}$$

$$h = c_p T. \tag{5}$$

The functional dependencies of the first and second coefficients of viscosity, μ and λ, the thermal conductivity K, the mass diffusion coefficient D, and the reaction rates R_l, are assumed to be known, although the specific form of these dependencies is immaterial for the derivations of this section.

Beginning with these basic equations, our strategy will be to derive an approximate set of equations based on either the low Mach number or high Reynolds number assumption. It will then be demonstrated that these approximate equations remain invariant under certain transformations of the dependent and independent variables.

Derivation of the α-Transformation

We first use an order-of-magnitude estimate for terms in the momentum equation (2) to show that the pressure is nearly uniform if certain conditions are satisfied, the principal one being that the Mach number is small. Let

$$\begin{aligned} \hat{t} &= t/t_0, \\ \hat{\mathbf{x}} &= \mathbf{x}/L, \\ \hat{\mathbf{u}} &= \mathbf{u}/u_0, \\ \hat{\rho} &= \rho/\rho_0, \\ \hat{\mu} &= \mu/\mu_0, \end{aligned}$$

where characteristic quantities t_0, L, u_0, ρ_0, and μ_0 are chosen in such a way that $\hat{\rho}$, $\hat{\mathbf{u}}$, $\hat{\mu}$, and their derivatives with respect to $\hat{t}$ and $\hat{\mathbf{x}}$ are all of the order of unity. The nondimensionalized momentum equation becomes

$$\frac{L}{u_0 t_0}\frac{\partial \hat{u}}{\partial \hat{t}} + \hat{\mathbf{u}} \cdot \nabla_{\hat{x}}\hat{\mathbf{u}} + \frac{P_0}{\rho_0 u_0^2}\frac{1}{\hat{\rho}}\frac{\nabla_{\hat{x}} P}{p_0} = \frac{\mu_0}{\rho_0 u_0 L}\frac{1}{\hat{\rho}}\nabla_{\hat{x}} \cdot \hat{\underline{\tau}}, \tag{6}$$

where p_0 is a characteristic value of the pressure. Three assumptions are made:

$$\frac{u_0^2 \rho_0}{p_0} \approx M^2 \ll 1, \tag{A1}$$

$$St = \frac{L}{u_0 t_0} \leqslant O(1), \tag{A2}$$

$$Re = \frac{\rho_0 u_0 L}{\mu_0} \geqslant O(1). \tag{A3}$$

Then, since every term in (6) is at most of order unity, we have

$$\frac{|\nabla_{\hat{x}} p|}{p_0} = O(M^2) \ll 1;$$

that is, departure of the pressure from its mean value is small over a distance L. If the

entire flow region can be subdivided into a small number of subregions of dimension L_i, in each of which the above inequalities hold, then we have in addition

$$\frac{|\delta p|}{p_0} \ll 1, \tag{7}$$

where δp is the difference in pressure between any two points in the flow field. Let $\bar{p}(t)$ be the volume averaged pressure and

$$p'(\mathbf{x}, t) = p(\mathbf{x}, t) - \bar{p}(t)$$

the pressure fluctuation. Further order-of-magnitude estimates based on (6) and (A1) show that the pressure fluctuation and viscous dissipation terms in Eq. (3) and the pressure fluctuation term in (4) may be neglected. The momentum equation, equation of state, and energy equation then become

$$\frac{\partial \mathbf{u}}{\partial t} + \mathbf{u} \cdot \nabla \mathbf{u} + 1/\rho \, \nabla p' = 1/\rho \, \nabla \cdot \underline{\tau}, \tag{8}$$

$$\bar{p} = \frac{\gamma - 1}{\gamma} \rho h, \tag{9}$$

and

$$\frac{\partial \rho h}{\partial t} + \nabla \cdot (\rho \mathbf{u} h) = \frac{d\bar{p}}{dt} + \nabla \cdot (K \nabla T) + \sum_i R_i Q_i \,. \tag{10}$$

One further equation of change for $\bar{p}(t)$ will be used, and this is derived taking into account the boundary conditions of the problem. For the applications considered in this paper—combustion in a closed chamber of fixed dimensions—the following boundary conditions are used:

$$\mathbf{u} \cdot \mathbf{n}\,|_{\text{wall}} = 0, \tag{11}$$

$$\left.\frac{\partial \mathbf{u} \cdot \mathbf{t}}{\partial \mathbf{n}}\right|_{\text{wall}} = 0 \qquad \text{(free-slip walls)}, \tag{12}$$

$$\left.\frac{\partial T}{\partial \mathbf{n}}\right|_{\text{wall}} = 0, \tag{13}$$

$$\left.\frac{\partial}{\partial \mathbf{n}}\left(\frac{\rho_k}{\rho}\right)\right|_{\text{wall}} = 0, \tag{14}$$

where $\mathbf{n}$ is the unit outward normal and $\mathbf{t}$ a unit tangent vector to the wall. By (12) and (13), we are ignoring momentum and energy losses in wall boundary layers. Although the validity of the α-transformation will be demonstrated for these boundary conditions, it can be verified that the transformation remains valid for a variety of different boundary conditions, including: (i) no-slip, constant-temperature walls,

(ii) closed volume with prescribed wall motion (provided the wall velocity is scaled properly), and (iii) unconfined combustion in the open atmosphere.

Multiplying Eq. (10) by $(\gamma - 1)/\gamma$, using (9), and solving for $d\bar{p}/dt$ yields

$$\frac{d\bar{p}}{dt} + \gamma \bar{p} \nabla \cdot \mathbf{u} = (\gamma - 1) \left\{ \nabla \cdot (K \nabla T) + \sum_l R_l Q_l \right\}. \tag{15}$$

Integrating (15) over the confining volume V and using (11) and (13) gives the result

$$\frac{d\bar{p}}{dt} = \frac{\gamma - 1}{V} \int_V \sum_l R_l Q_l \, d\tau. \tag{16}$$

With $d\bar{p}/dt$ given by (16), Eq. (15) may be viewed as an equation for the divergence of the velocity field. Equations (1), (5), (8), (9), (15), and (16) are the approximate equations governing low Mach number flows.

Care must be exercised in specifying proper initial conditions for the equations due to their elliptic nature. Once the thermodynamic variables have been specified, the divergence of the velocity field is determined by Eq. (15). We are free to specify only the initial vorticity field, which must, of course, be solenoidal. Accordingly, the initial conditions will be the following:

$$\bar{p}(0) = p_0 , \tag{17}$$

$$\rho_k(x, 0) = \rho_{k_0}(\mathbf{x}), \tag{18}$$

$$\boldsymbol{\zeta}(\mathbf{x}, 0) = \boldsymbol{\zeta}_0(\mathbf{x}), \tag{19}$$

where $\boldsymbol{\zeta}$ is the vorticity.

Under the one-parameter α-transformation, the dependent and independent variables are scaled in the following manner:

$$\begin{aligned} \mu^* &= \alpha\mu, \\ \lambda^* &= \alpha\lambda, \\ K^* &= \alpha K, \\ D^* &= \alpha D, \\ R_l^* &= \alpha R_l , \\ t^* &= t/\alpha, \\ \mathbf{u}^* &= \alpha\mathbf{u}, \\ p'^* &= \alpha^2 p', \\ \boldsymbol{\zeta}_0^* &= \alpha\boldsymbol{\zeta}_0 , \end{aligned} \tag{20}$$

where the superscript asterisk denotes the transformed variables. All other variables

remain unaffected by the transformation. The parameter α must, in general, be a constant.

It will now be demonstrated that the approximate equations together with the specified boundary conditions (11)–(14) and initial conditions (17)–(19) remain invariant under the α-transformation. It is easy to verify that the equations remain invariant. For example, when the transformation is applied to the momentum equation (8), the result is

$$\frac{1}{\alpha^2}\frac{\partial \mathbf{u}^*}{\partial t^*} + \frac{1}{\alpha^2}\mathbf{u}^* \cdot \nabla \mathbf{u}^* + \frac{1}{\alpha^2}\frac{1}{\rho}\nabla p'^* = \frac{1}{\alpha^2}\frac{1}{\rho}\nabla \cdot \underline{\tau}^*$$

in which a factor $1/\alpha^2$ multiplies each term. The boundary conditions remain invariant since they are homogeneous. To show that the initial conditions remain invariant, one must show that the velocity field which is determined by $\zeta_0 = \alpha\zeta_0$ and $(\nabla \cdot \mathbf{u})^*_{t=0} = \alpha(\nabla \cdot \mathbf{u})_{t=0}$ is identical to α times the original initial velocity field. But these velocity fields have identical divergence and vorticity and hence must be the same.

Note that all diffusivities and reaction rates are multiplied by the factor α, and that the Mach number is scaled by a factor of α while the Reynolds number remains invariant. This is consistent with classical formulas [1] for flame speed and thickness, which predict that when the diffusivities and reaction rates are increased by a factor of α, the flame speed will increase by α while the flame thickness will remain unchanged.

The solution to the complete equations (1)–(5) using the scaled diffusivities and reaction rates will be close to the solution of the approximate equations of this section, as long as conditions (A1)–(A3) are satisfied by the scaled characteristic quantities. Substituting from (20) into (A1)–(A3) gives

$$M^{*2} = \alpha^2 M^2 \ll 1 \tag{21}$$

as the only condition for this to be true (as long as (A2) and (A3) are satisfied by the unscaled variables). Hence the transformation will be valid as long as (21) is satisfied, although a more precise upper bound for α must be determined by numerically solving the complete equations (1)–(5) and varying the value of α as it is shown in a later section.

Computational time saving is realized because the sound speed c remains unchanged while the total problem time τ is scaled by a factor of $1/\alpha$. In traditional hydrodynamics codes for the solution of compressible flows, the Courant sound speed restriction on the magnitude of the computational time step $(|u| + c)\,\delta t/\delta x < 1$ must be observed. In low-speed flows, since $c^* = c$, the time step δt^* used in solving the transformed problem can be taken to be nearly equal to δt. Since for the transformed problem

$$\tau^* = \tau/\alpha,$$

it is seen that the number of computational time steps needed to achieve solution of the entire problem is reduced by a factor of $1/\alpha$. In our applications, we used a

computer program employing the ICE technique [4], which obviates the need to observe the Courant sound speed restriction. The limiting criterion on the magnitude of the time step in our applications is that for diffusional stability:

$$D\,\delta t/\delta x^2 < \tfrac{1}{4}.$$

Since $D* = \alpha D$, we have to take $\delta t = \delta t/\alpha$. Nevertheless, computational timesavings is still realized since in the iterative procedure used in ICE to solve the acoustic wave motion, the number of iterations is proportional to the distance a sound wave must travel in one time step. Since $c* \,\delta t* = c\,\delta t/\alpha$, the number of iterations is reduced by a factor of $1/\alpha$.

Derivation of the β-Transformation

The general idea behind the β-transformation, that the flame zone can be artificially thickened to the dimensions of the computational mesh, was first presented by Butler and O'Rourke [7]. Our objective here is to examine the assumptions needed for the validity of the β-transformation more carefully. The major assumption is that the thickness of the flame is much smaller than any other characteristic length of the flow; that is,

$$\delta \ll L, \tag{B1}$$

where the reference length L is the smallest of such lengths as the dimension of the chamber, the local radius of curvature of the flame, and the characteristic lengths of possible nonuniformities in the flow field away from the flame. Although we do not define the flame thickness δ here, there is usually little doubt, in practice, when assumption (B1) is satisfied.

Assumption (B1) implies that the flame front may be approximated as a discontinuity in an inviscid, nonconducting, nondiffusive mixture of gases. Indeed, within a flame with a flame velocity u_f, convection and diffusion times are of the same order [1], implying

$$t_{\text{conv}} \approx \delta/u_f$$

and

$$t_{\text{diff}} \approx \delta^2/D \tag{22}$$

and hence

$$D \approx \delta u_f .$$

The maximum induced gas velocity, u, is given by [1]

$$u \approx u_f \frac{Q}{c_p T_0},$$

where Q is the heat release per mass of reactant and T_0 is the temperature ahead of the flame. In practice, $Q/c_pT_0 > 1$. Recalling that for gaseous mixtures, $Sc = \mu/\rho D = O(1)$, it follows that

$$\begin{aligned} Re &= \frac{\rho u L}{\mu} \\ &= \frac{\rho D}{\mu}\frac{u}{u_f}\frac{u_f}{D}L \\ &> O(L/\delta) \gg 1. \end{aligned} \tag{23}$$

In addition to assumption (B1), we will have to require that the mixture away from the flame be either chemically frozen or in equilibrium; that is,

$$t_{\text{ch}} \ll L/u \qquad \text{(equilibrium flow)} \tag{B2a}$$

or

$$t_{\text{ch}} \gg L/u \qquad \text{(frozen flow)}, \tag{B2b}$$

where t_{ch} is a characteristic chemistry time.

Nondimensionalizing the variables in Eqs. (1)–(6) by our reference parameters, using (23) and either (B2a) or (B2b), and recalling that for gases, $Pr \approx Sc \approx 1$, one deduces the following well-known equations for the flow ahead of and behind the flame front:

$$\begin{aligned} \frac{\partial \mathbf{u}}{\partial t} + \mathbf{u}\cdot\nabla\mathbf{u} + \frac{1}{\rho}\nabla p &= 0, \\ \frac{\partial \rho h}{\partial t} + \nabla\cdot(\rho\mathbf{u}h) &= \frac{\partial p}{\partial t} + \mathbf{u}\cdot\nabla p; \end{aligned} \tag{24}$$

frozen:

$$\frac{\partial \rho_k}{\partial t} + \nabla\cdot(\rho_k\mathbf{u}) = 0 \qquad \left(\text{or } \frac{D\rho_k/\rho}{Dt} = 0\right);$$

equilibrium:

$$\frac{\partial c_a}{\partial t} + \nabla\cdot(c_a\mathbf{u}) = 0 \qquad \left(\text{or } \frac{D\rho_a/\rho}{Dt} = 0\right)$$

and

$$\sum_k \nu_k{}^a c_k = c_a$$

and

$$R_l{}^f = R_l{}^b,$$

where

$$c_a = \text{moles of atom } a \text{ per unit volume},$$
$$c_k = \text{moles of molecule } k \text{ per unit volume},$$
$$\nu_k{}^a = \text{number of atoms of type } a \text{ in molecule } k,$$

and $R_l{}^f$ and $R_l{}^b$ are the forward and backward reaction rates of reaction l.

In the frame of reference of the flame, the equations which govern the flow in the flame zone are those for a planar, one-dimensional, steady combustion wave propagating into a uniform mixture. This can be seen by writing the governing equations in a boundary-layer coordinate system which moves with the flame. Assumption (B1) implies that gradients in the field variables in a tangent direction can be neglected in comparison to those normal to the flame and that curvature effects can be ignored. Also

$$\delta/u_0 \ll L/u_0 , \tag{25}$$

where u_0 is a characteristic velocity. Equation (25) says that the residence time in the flame is much smaller than a characteristic time for changes in the fluid variables. This, in turn, implies that the flow in the flame zone is quasi-steady and that we can neglect acceleration terms which arise due to our non-Galilean frame of reference. With x being the coordinate normal to the flame and u the fluid velocity in the x-direction, the approximate equations for the flow in the flame zone become

$$\frac{\partial}{\partial x}(\rho_k u) = \frac{\partial}{\partial x}\left(\rho D \frac{\partial Y_k}{\partial x}\right) + W_k \sum_l R_l(\nu''_{k,l} - \nu'_{k,l}), \tag{26}$$

$$\frac{\partial}{\partial x}(\rho u^2 + p) = \frac{\partial}{\partial x}\left[(2\mu + \lambda)\frac{\partial u}{\partial x}\right] \tag{27}$$

and

$$\frac{\partial}{\partial x}(\rho u h) = u\frac{\partial p}{\partial x} + \frac{\partial}{\partial x}\left(K\frac{\partial T}{\partial x}\right) + (2\mu + \lambda)\left(\frac{\partial u}{\partial x}\right)^2 + \sum_l R_l Q_l . \tag{28}$$

Having been divided into outer and flame regions, which are governed by Eqs. (24) and (26)–(28), together with equations of state (4) and (5), the flow field is then reconstructed by specifying that the conditions to be satisfied immediately ahead of and behind the discontinuity in the outer solution should be those which are satisfied at $x = -\infty$ and $x = +\infty$ by the inner flame region. These interface conditions are, of course, the mass burning rate and the Rankine–Hugoniot relations. In addition, the boundary condition along rigid walls is

$$\mathbf{u} \cdot \mathbf{n}_{\text{wall}} = 0, \tag{29}$$

and the initial conditions are specification of pressure, density, and velocity fields consistent with boundary condition (29) and the interface conditions.

The β-transformation can be viewed as an expansion of the coordinate normal to the burn front. With $\beta(x)$ an expansion factor, let

$$\begin{aligned} x^* &= \int^x \beta(x')\,dx', \\ D^* &= \beta D, \\ \mu^* &= \beta\mu, \\ \lambda^* &= \beta\lambda, \\ K^* &= \beta K, \\ R_i^* &= R_i/\beta. \end{aligned} \tag{30}$$

All other variables are unaffected by the transformation.

It is easy to verify that the approximate equations remain invariant under the transformation. For frozen flow, Eqs. (24) are inviscid with no chemical reaction and hence are unaffected by the transformation. For flow in chemical equilibrium, the effect of multiplying both the forward and backward reaction rates by $1/\beta$ cancels out of the equation. Also initial and boundary conditions, which are specified for the outer regions, are not affected. For the enthalpy equation (28), we have

$$\beta \frac{\partial}{\partial x^*}[\rho u h] = u\beta \frac{\partial p}{\partial x^*} + \beta \frac{\partial}{\partial x^*}\left(K^* \frac{\partial T}{\partial x^*}\right) + \beta(2\mu^* + \lambda^*)\left(\frac{\partial u}{\partial x^*}\right)^2 + \beta \sum_i R_i^* Q_i$$

in which a factor β appears in each term. Equations (26) and (27) can similarly be verified to remain invariant.

In contrast to the α-transformation, the diffusivities are multiplied by β, the reaction rates are divided by β, the Mach number remains invariant, and the Reynolds number is decreased by a factor $1/\beta$. This is also consistent with classical formulas for the flame speed thickness [1], which predict that under these circumstances the flame speed will remain unchanged, while the flame thickness will increase by a factor β.

The solution to the approximate equations of this section will be close to the solution of the complete equation (1)–(5) as long as the transformed flame thickness satisfies (B1). Since the solution to the approximate equations is independent of β, except that the flame thickness is altered, solutions to the complete equations should be close to each other as long as

$$\delta* \ll L. \tag{31}$$

To determine a more precise upper bound for $\delta*$, we will solve the complete equations numerically and vary the value of β.

Computational time saving is realized because the number of computational cells can be reduced. In a calculation in two space dimensions, for instance, if the burn zone

thickness is increased by a factor β, the computational cell size $\delta x*$ for the transformed problem can be taken as

$$\delta x* = \beta \, \delta x$$

and the number of computational cells is reduced by a factor $1/\beta^2$.

In the following section, we will describe, in detail, how both transformations have been used to compute the propagation of a premixed, laminar flame in a closed chamber.

Computational Results

The calculations, which were performed to test the validity and range of applicability of the scaling transformations, were made with the computer coce RICE [8]. RICE solves the complete two-dimensional, unsteady equations of change for a chemically reacting mixture of ideal gases. It employs a fixed, Eulerian computational grid of uniform cell size and uses the ICE technique.

The computational parameters were selected to simulate an experiment performed at Volkswagen R&D in a constant volume vessel [9]. Although in this paper, the computed results are not compared with the measured ones, we briefly describe here the geometry and initial conditions of the experiment in order to justify our choice of the computational parameters. The Volkswagen combustion bomb, is depicted schematically in Fig. 1. The top and bottom walls are glass windows through which high-speed Schlieren filming of the combustion event is made. In the experiment, for which data were supplied by Volkswagen R&D, the charge was a stochiometric methane–air mixture at an initial pressure of 3 atm and temperature of 450°K. The initially quiescent mixture was spark ignited at the side wall. After a short initial period during which the flame propagated outward to the top and bottom walls, a

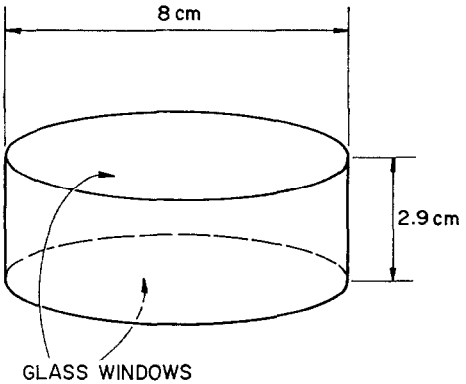

Fig. 1. Schematic diagram of the Volkswagen combustion bomb.

nearly two-dimensional flame was observed in Schlieren photographs. The total combustion time of 40 msec was of the order one would expect from reported laminar flame speeds of methane–air mixtures [10]. For such laminar flames, the assumptions needed for both the α- and β-transformations are well satisfied.

Figure 2 depicts the geometry used in the calculations. The circular cross section of the bomb is approximated with an octagon, and the symmetry of the experiment has

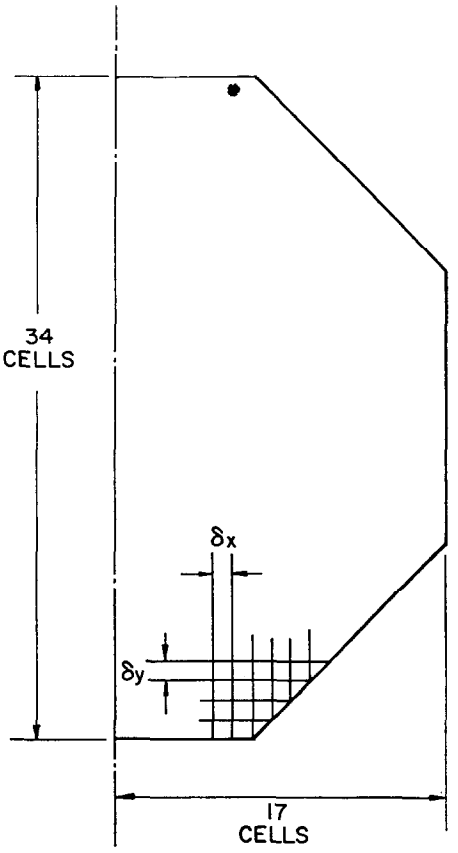

FIG. 2. Finite-difference mesh used in the calculations.

been exploited to halve the combustion chamber and the computational time. The computational cells were of uniform size, $\delta x = \delta y = 0.23$ cm, in all calculations except one, in which $\delta x = \delta y = 0.115$ cm was needed to resolve the flame adequately. The chemistry and species data used in the calculations are given in Table I. A simplified one-step kinetics model was employed with a heat release Q reduced by 15% from the heat of complete combustion of methane and air, to take into very rough account effects of dissociation and wall heat transfer. The specific heats of the reactant species A and product species B, which were constant, were taken to be

TABLE I

Chemistry and Species Data

Species	c_v (ergs/g-°K)	γ	W (g/mole)
A	7.54×10^6	1.39	27.62
B	1.01×10^7	1.29	27.62

Reaction: $A \rightarrow B + Q$

$$\frac{d[A]}{dt} = -[A]^2 c_f \exp\left[-\frac{E_f}{T}\right]$$

$c_f = 1.0 \times 10^{15}$ cm³/mole-sec

$E_f = 20{,}000$°K

$Q = 7.19 \times 10^{11}$ ergs/mole reactant

$\mu = 1.34 \times 10^{-5} T^{1/2}$ g/cm-sec

$Pr = Sc = 0.75$

those of nitrogen at 450°K and 2400°K, respectively. The shear viscosity μ was taken to be

$$\mu = 1.34 \times 10^{-5} T^{1/2} \qquad \text{g/cm-sec},$$

which closely approximates the viscosity of air in the temperature range under consideration. The heat conduction and mass diffusion coefficients were computed from $Pr = Sc = 0.75$, and $\lambda = \mu$ was adopted.

The initial conditions used in the calculations are summarized in Fig. 3. The initial flame position was chosen to match that observed in the experiment approximately

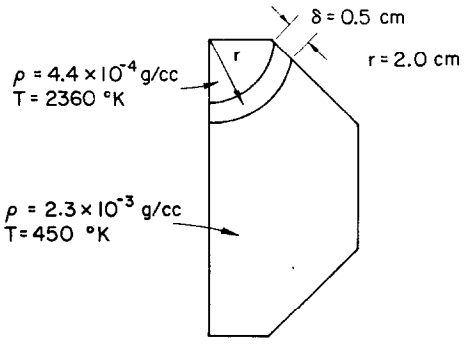

FIG. 3. Initial conditions used in the calculations.

10 msec after ignition. Estimated temperature and species profiles within the flame front were set in a strip 0.5 cm thick and located 2 cm from the ignition site. Ahead of the flame the temperature was 450°K, while in the burned mixture the temperature was 2360°K. The initial pressure was 3 atm and the fluid velocities were set to zero. The boundary conditions were adiabatic, free-slip walls. We note here that neglect of wall momentum and energy losses is consistent with our earlier assumption that the flow outside of the flame zone is approximately invisicid.

The starred values for the diffusivities and reaction rates used in the calculations were

$$\mu^* = \alpha\beta\mu,$$
$$\lambda^* = \alpha\beta\lambda,$$
$$K^* = \alpha\beta K,$$
$$D^* = \alpha\beta D,$$
$$R_i^* = \alpha R_i/\beta.$$

The form for β, which can vary in space and time, was taken to be

$$\beta = \rho\Delta/\mu,$$

where $\Delta \equiv$ constant. This results in a constant value for the diffusivities; for example,

$$\frac{\mu^*}{\rho} = \frac{\alpha\beta\mu}{\rho} = \alpha\Delta.$$

The values of α and β were varied independently in the parametric study. With $\beta = \beta_0 = 50\rho/\mu$, four calculations were made using values of $\alpha = 1$, 10, 25, and 100, and with $\alpha = 10$, three calculations were performed with $\beta = \frac{1}{2}\beta_0$, β_0, and $2\beta_0$. Some of the results of these calculations are summarized in Table II.

In the calculations in which α was varied, it is seen that increasing α resulted in a decrease in computational time of nearly a factor of 3. The Mach numbers in the last column are the maximum Mach numbers seen in computer printouts at intermediate times in the calculations. In all calculations except that for which $\alpha = 100$, the predicted dependence of the transformed Mach number on α was satisfied. In the $\alpha = 100$ calculation a rapid rise in the pressure occurred and supersonic velocities were observed. The conditions for the validity of the α-transformation had been violated as shown by the fact that the computed Mach number was much higher than the expected one of $M^{*2} = 0.15$.

The pressure as a function of the untransformed time for the various values of α is plotted in Fig. 4. On the scale of the graph, the calculations with $\alpha = 1$ and 10 resulted in identical pressure histories. When α was raised to 25, oscillations were superimposed on the overall rise in pressure; the timing of the oscillations correlated with that for acoustic wave travel across the chamber and back again. From the runs with $\alpha = 25$

TABLE II

Parametric Study

$\beta_0 = 50\rho/\mu_{\text{true}}$

α	δt (sec)	Computational time[b] (min)	M^{*2}
1	5×10^{-5}	22.8	1.5×10^{-5}
10	5×10^{-6}	12.3	1.5×10^{-3}
25	2×10^{-6}	8.3	9.4×10^{-3}
100	5×10^{-7}	8.0	?

$\alpha = 10$

β	δt (sec)	Computational time[b] (min)	(cm)
$\frac{1}{2}\beta_0$ [a]	2.5×10^{-6}	86	0.4
β_0	5×10^{-6}	12.3	0.8
2β	2.5×10^{-6}	14.0	1.6

[a] $\delta x = \delta y = 0.115$ cm.
[b] IBM 360/91.

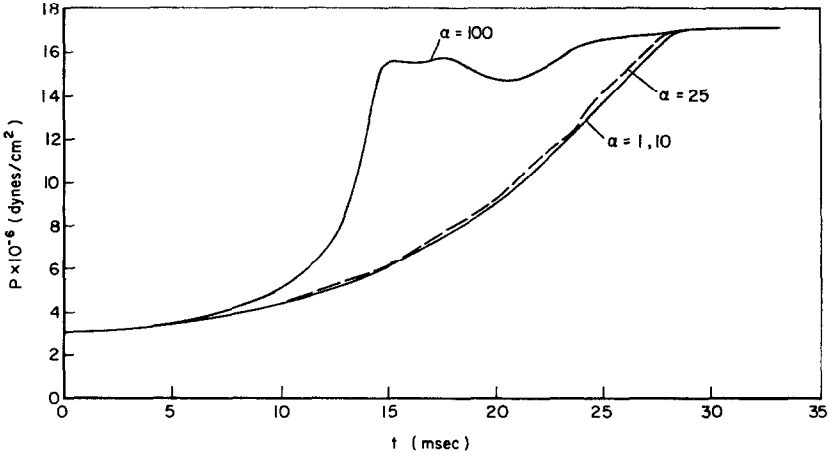

FIG. 4. Pressure histories showing affects of varying α for fixed $\beta = \beta_0 = 50\rho/\mu$.

and $\alpha = 100$, it was inferred that the α-transformation becomes invalid for $M*^2$ between 0.01 and 0.15.

Table II also shows the saving in computer time which is realized when β is increased. In the calculation for which $\beta = \frac{1}{2}\beta_0$, the mesh had to be refined by a factor of 2 to resolve the flame, and the time step also had to be halved. This resulted in nearly a factor of 8 increase in the computational time. The flame thickness $\delta*$ in the right-hand column is an average thickness inferred from temperature contour plots made by the computer program. Again the predicted dependence of the flame thickness on the value of β is confirmed. Representative isotherm plots are displayed in Fig. 5.

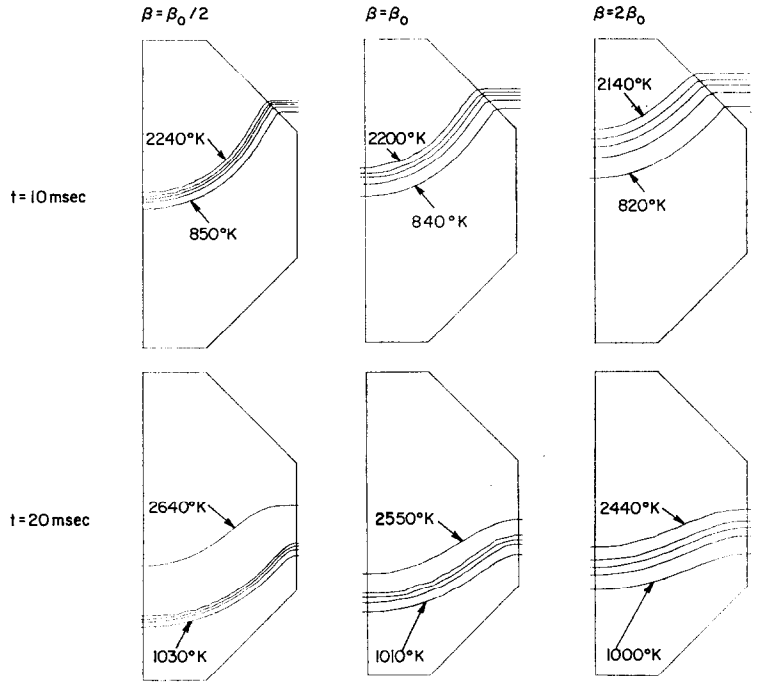

FIG. 5. Comparison of temperature contour plots at two different times for the three calculations in which β was varied.

In Fig. 6 are shown the pressure histories of the three calculations with β varying. The three curves are seen to be in substantial agreement, with the small discrepancies near the end of the calculations attributable to the fact that the thicker flames in the larger β cases "see" the wall sooner. The curves have been drawn so that their common origin is that time at which the pressure reached 5 atm. Although the flame thickness is different in the three calculations, the same initial guess for the flame thickness was used in each case. Hence there is a short time, which will be different for each calculation, during which the flame profiles will relax to their quasi-steady values. In order that this not influence the comparison, we have taken the computed profiles at 5 atm as new initial conditions.

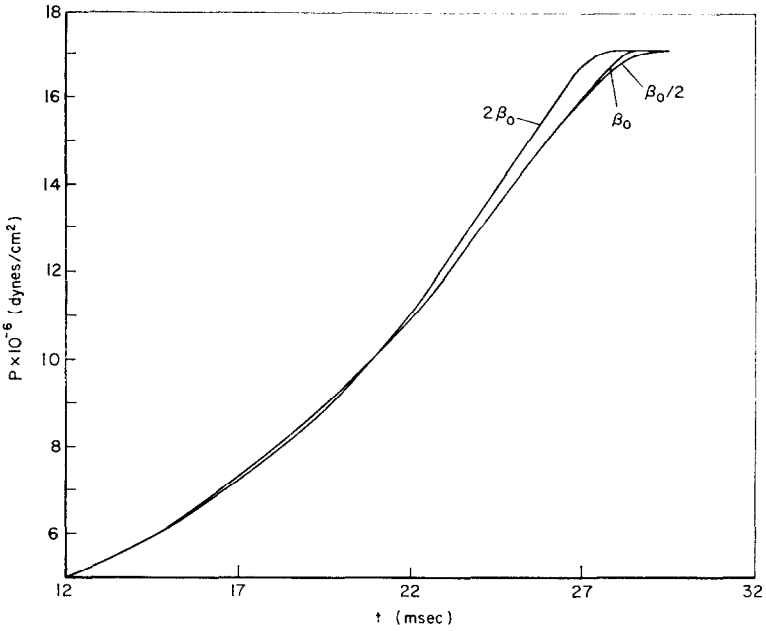

FIG. 6. Pressure histories showing the affects of varying β for fixed $\alpha = 10$.

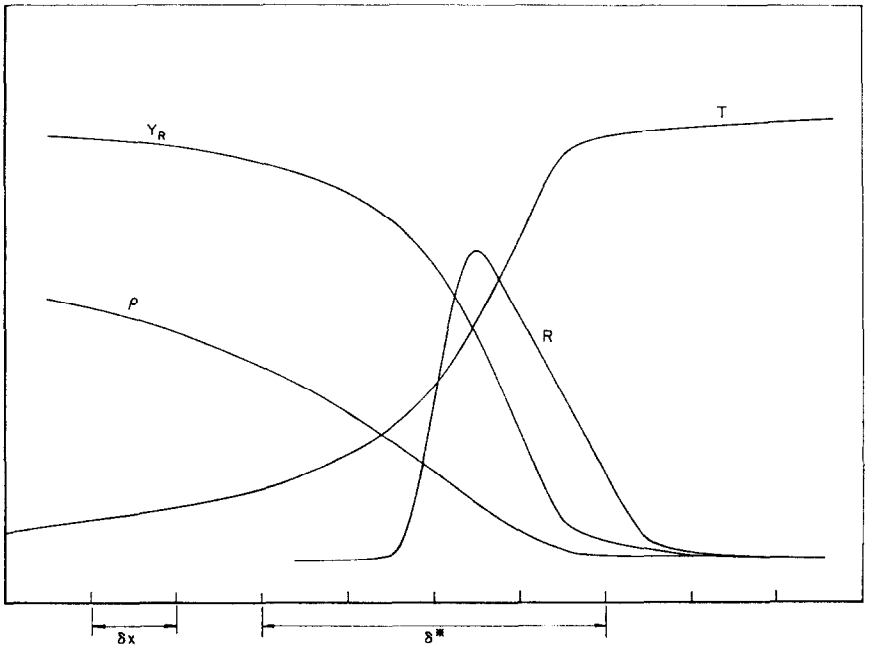

FIG. 7. Selected flame variables obtained at $t = 18$ msec in the calculation for which $\alpha = 10$ and $\beta = 50\rho/\mu$.

Representative profiles of the temperature, density, fuel mass fraction, and reaction rate through a cross section of the flame front are displayed in Fig. 7. It can be seen that the flame is resolved with about four computational cells, corresponding to $\delta* = 1.0$ cm. Since the diameter of the chamber is 8.0 cm, good agreement is seen despite the fact that $\delta*/L > 1/8$.

In general, $\delta*$ must be large enough to resolve the flame front, but small enough to satisfy the condition $\delta* \ll L$. In any numerical study, then, the value of β, and also of α, should be varied in order to test the results for invariance as was done in this section of our study.

Summary

Two scaling transformations have been discussed and verified which make possible the calculation of multidimensional, unsteady laminar flames.

The primary assumption needed for the α-transformation is that of low Mach number flow. In this transformation, the diffusivities and reaction rates are multiplied by α and the time is scaled by a factor $1/\alpha$. Scaling of initial velocities and wall boundary velocities is also required.

For the β-transformation, the flame thickness must be small compared to any other characteristic length of the problem. The diffusivities are multiplied by β and the reaction rates by $1/\beta$. The transformation only affects the solution in the flame front by increasing the flame thickness by a factor of β without changing the flame speed, and boundary conditions need not be scaled.

Acknowledgments

Support for this research was provided by the Department of Energy, Contract EC-77-S-02-4191, Dr. J. Birkeland, Technical Monitor, and by the National Science Foundation, Grant 77-12142, Dr. R. Rostenbach, Grant Monitor.

References

1. F. A. Williams, "Combustion Theory," pp. 95–111, Addison–Wesley, Reading, Mass., 1965.
2. S.-I. Pai, "Viscous Flow Theory," Vol. 1, p. 206, Van Nostrand, Princeton, N. J., 1956.
3. J. von Neumann and R. D. Richtmyer, *J. Appl. Phys.* **21** (1950), 232–237.
4. F. H. Harlow and A. A. Amsden, *J. Computational Phys.* **8** (1971), 197–213.
5. F. H. Harlow and J. E. Welch, *Phys. Fluids* **8** (1965), 2182.
6. C. W. Hirt, A. A. Amsden, and J. L. Cook, *J. Computational Phys.* **14** (1974), 227–253.
7. T. D. Butler and P. J. O'Rourke, *in* "Proceedings, Sixteenth Symposium on Combustion August, 1976," pp. 1503–1516, The Combustion Institute, Pittsburgh, 1977.
8. W. C. Rivard, O. A. Farmer, and T. D. Butler, Los Alamos Scientific Laboratory Report LA–5812, November 1974.
9. W. R. Brandstetter and R. Decker, *Combustion and Flame* **25** (1975), 15–23.
10. B. Lewis and G. von Elbe, "Combustion, Flames, and Explosions of Gases," p. 389, Academic Press, New York, 1961.